2950 Niles Road, St. Joseph, MI 49085-9659, USA
269.429.0300 fax 269.429.3852 hq@asabe.org www.asabe.org

An ASABE Meeting Presentation
DOI: https://doi.org/10.13031/aim.201701593
Paper Number: 1701593

Better Almond Water Stress Monitoring Using Fractional-order Moments of Non-normalized Difference Vegetation Index

Tiebiao Zhao[1], David Doll[2], Dong Wang[3], YangQuan Chen[1]
[1]University of California, Merced

[2]University of California, Cooperative Extension, Merced

[3]USDA-ARS Water Management Research Unit, San Joaquin Valley Agricultural Sciences Center, Parlier, CA

Written for presentation at the
2017 ASABE Annual International Meeting
Sponsored by ASABE
Spokane, Washington
July 16-19, 2017

ABSTRACT. ***Stem water potential (SWP) has become a very popular tool for farmers to monitor the water status of almond trees. However, it is labor intensive and time consuming to scale up the measurements in the large field. With the development of unmanned aerial vehicles (UAVs) and sensing payload, it becomes possible to monitor the water status much more efficiently with UAV-based multispectral images of higher spatial resolution and more flexible temporal resolution. Driven by this possibility, studies have been started in a commercial almond orchard since 2014 to research almond water stress monitoring using the small unmanned aerial vehicle and the modified multispectral camera. More specifically, we are researching how to predict almond SWP by extracting information from these multispectral images. Recent experiments showed that traditional vegetation indices such as normalized difference vegetation index (NDVI) do not work very well with high resolution aerial images to predict SWP. Meanwhile, we found non-normalized difference vegetation index (NNDVI) between near-infrared (NIR) band, blue band, and its higher order moments have a better correlation with SWP. In this paper, we proposed the fractional-order moments of NNDVI and discussed its correlation with SWP. It is shown that the correlation between the proposed fractional-order moments of NNDVI and SWP is more significant than that between the traditional NDVI and SWP.***

Keywords. ***Water stress detection, unmanned aerial vehicles (UAVs), stem water potential (SWP), fractional-order moments, non-normalized difference vegetation index (NNDVI)***

Introduction

Water is one of the major constraints all around the world in agriculture. As one of the top three challenges, water scarcity is affecting two-thirds of world's population up to a month a year (Mekonnen & Hoekstra, 2016). Plants will experience water stress if evaporative demand is more than water supply in the soil (Slayter & others, 1967). Under water

stress, crops will close stomata and reduce uptake of carbon dioxide and their growth will be diminished (Nilsson, 1995). As one of the most important crops in California, almond uses 9.5 percent of the states' water in agriculture. Water stress will cause a reduction of kernel size and number of nuts and hence serious yield production losses (Steduto, Hsiao, Fereres, & Raes, 2012; Shackel, et al., 2011; Doll & Shackel, 2016). In addition, it will affect future floral bud development and cause compound losses (Doll & Shackel, 2016).

To ameliorate the water usage without sacrificing yield, it is critical to optimize irrigation schedules and apply water in the right amount and at the right time. The success of optimizing irrigation schedules depends on how easily growers can measure water stress in the fields. Currently, proper irrigation scheduling is based on soil moisture status, evaporative demand and plant water status (Steduto, Hsiao, Fereres, & Raes, 2012). Plant based water status measurement provides an integrated view of plant-soil continuum (Dhillon, Francisco, Roach, Upadhyaya, & Delwiched, 2014). SWP has been proven to be a useful index in many fruit species and able to indicate short- and medium-term plant response to stress (Shackel, et al., 1997) and serves as the standard method for plant water status monitoring. Instructions for scheduling irrigation based on SWP have been developed (Shackel, Lampinen, Sibbett, Olson, & others, 2000). However, it has not been well adopted in irrigation practice. This is mainly because SWP measurement is very labor intensive and time consuming, requiring the sampling time either during pre-dawn or within 2 hours around solar noon, and about 3–5 minutes per sample (Shackel, Lampinen, Sibbett, Olson, & others, 2000). This makes it almost impossible to conduct the measurements for the whole field.

Remote sensing provides the capability of real-time measurement in a large scale. With the fast development of small unmanned vehicles systems (sUAS) and imaging payload, sUAS based remote sensing becomes more and more popular. Images can be collected with a lower cost, higher-spatial resolution and flexible timing, spurning a lot of research on applications of water stress monitoring using sUAS. Crop water stress index (CWSI) correlated well with SWP in peach trees (Wang and Gartung, 2010; (Bellvert, et al., 2016), pistachio trees (Goldhamer, Fereres, Mata, Girona, & Cohen, 1999) and almond trees (Gonzalez-Dugo, et al., 2012). Photochemical Reflectance Index (PRI) showed good correlation with SWP in olive trees (Suárez, Zarco-Tejada, González-Dugo, Berni, & Fereres, 2008). Non-normalized vegetation difference index was shown to have good correlation with SWP in almond trees (Zhao, Stark, Chen, Ray, & Doll, 2016).

It has been shown that, the average of vegetation indices such as NDVI is similar under different image resolutions, either obtained from satellites, sUAS or hand-hold scanners (Matese, et al., 2015; Zheng, et al., 2016). As a result, high resolution images will not benefit the final measurements if the average statistic is used. On the other hand, the temperature distribution within the individual canopy showed water stress (Gonzalez-Dugo, et al., 2012; Agam, et al., 2014) characterized by a positive skewness. Similarly, histogram shapes of NDVI are also used to compare stress levels at different regions (Candiago, Remondino, De Giglio, Dubbini, & Gattelli, 2015).

Inspired by these works, the goal of this study is to discuss the relationship between the higher order moments of vegetation indices and SWP. In particular, we extend the order of the moments from integer order to fractional order. Two different definitions of fractional-order moments are analyzed separately.

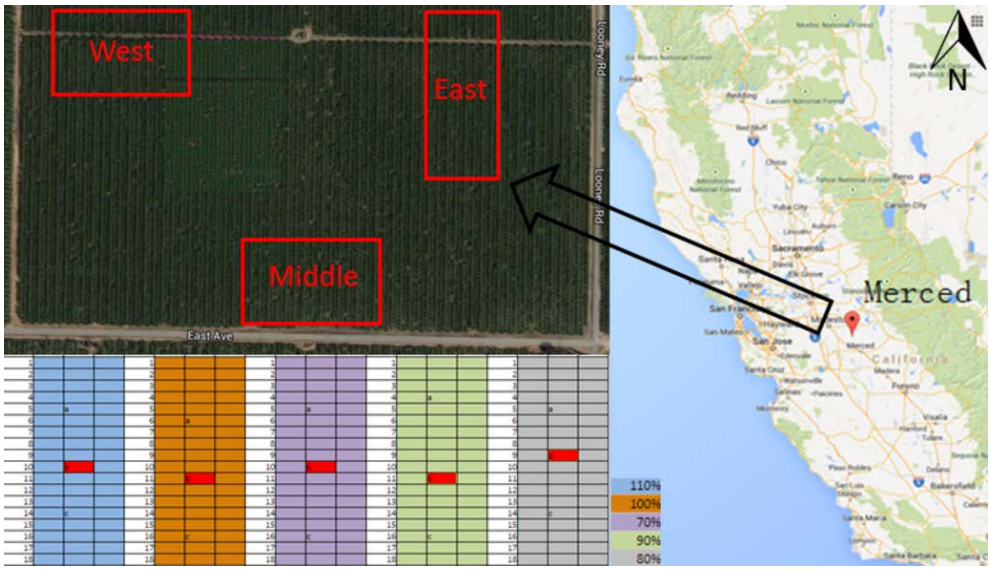

Figure 1. Test site overview

Material and Methods

Study Areas

The study site lies in a 15-year-old mature, commercial almond (Prunus dulcis) orchard in Merced County, California (37.493498◦N, -120.634914◦W). There are three varieties of almonds: Nonpareil, Carmel, and Monterey, all planted on Lovell peach rootstock, spaced at 5.5 m×6.1 m, with Rocklin loam and Greenfield sandy soil. The local climate is Mediterranean, characterized by wet, cool winters with a rainy season and hot, dry summers. Each block is treated with five different irrigation treatments, from 70% to 110% of crop evapotranspiration (ETc), with increment of 10%. Each treatment was replicated three times. Each plot is composed of three lines with 18 trees each and a buffer row between treatments (Fig. 1). Crop evapotranspiration was calculated according to the UN Food and Agriculture Origination (FAO) method (Allen, Pereira, Raes,Smith,&others,1998).

$$ET_c = K_c * ET_o \quad (1)$$

where ET_o is the reference evapotranspiration, and K_c is crop coefficient, defined as the ratio ET_c/ET_o.

Field Measurement

To determine the effects of irrigation treatments on tree water stress, midday SWP is measured using a pressure chamber ([1]PMS Instrument Model 600, Oregon, USA) following standard procedures (Fulton, Grant, Buchner, & Connell, 2014). These sample trees were measured once a week. The layout of sample trees is shown in Fig. 1, where the sample trees are marked with the letter a,b and c. SWP was measured simultaneously as the UAV flight campaigns.

Airborne Imagery

Two COTS (Commercial-off-the-shelve) cameras were flown from August, 2014 to October, 2015. One is configured to detect three bands: red, green, blue (RGB), and the other is configured to detect near-infrared (NIR), green, blue. Both cameras (ELPH110HS, Canon, Japan) have a resolution of 4608×3459 pixels with 24 bit radiometric resolution and a focal length 4.3mm. The modified NIR camera (LDP, LLC, USA) is centered at 430nm, 530nm and 700 nm with the quantum efficiency shown in Fig. 2.

Flight campaigns were conducted around noon at 60m altitude, yielding a ground spatial resolution of 1.87cm. The trigger distance for imaging was 16 m to generate vertical overlap up to 75%. Right before the flight missions, images of white panel were taken to convert digital number (DN) value of pixels to reflectance (Smith & Milton, 1999). Only the images of canopies taken with nadir angles were considered so the disturbance of bidirectional reflectance distribution function (BRDF) is minimized (Stark, Zhao, & Chen, 2016).

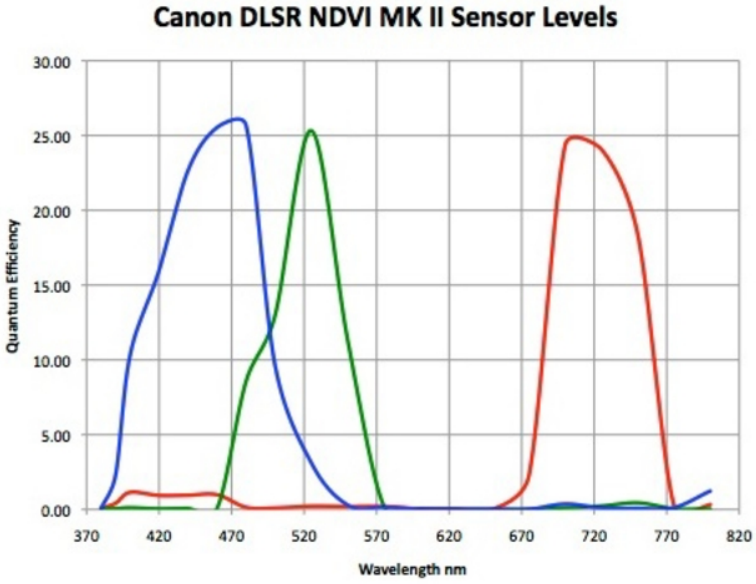

Figure 2. Band configuration of the modified NIR camera

[1] Mention of trade names or commercial products in this publication is solely for the purpose of providing specific information and does not imply recommendation or endorsement by the University of California or U.S. Department of Agriculture.

Fractional Order Moments

Considering a random sample X as $x_1, x_2, ..., x_N$, its standardized moments with order α defined as

$$\alpha_r = \frac{\mu_r}{\sigma_r} \tag{2}$$

where,

$$\mu_r = E\left[(X-\mu)^r\right] \tag{3}$$

$$\sigma_r = (E\left[(X-\mu)^2\right])^{r/2} \tag{4}$$

μ is the mean of this sample and r is an integer., To generalize the integer-order moments to fractional-order moments, r is set to be any real number. If $x_1-\mu, x_2-\mu, ..., x_N-\mu$ are positive, Eq.(2)-(4) can be easily generalized for any real number r. If it contains negative values, two calculation methods are proposed as fractional-order moment A

$$\alpha_{rA} = \frac{\mu_{rA}}{\sigma_r} \tag{5}$$

$$\mu_{rA} = E\left[(X-\mu)^r\right] = \frac{1}{N}\sum_{i=1}^{N}((x_i-\mu)^2)^{r/2} \tag{6}$$

and fractional-order moment B

$$\alpha_{rB} = \frac{\mu_{rB}}{\sigma_r} \tag{7}$$

$$\mu_{rB} = E\left[(X-\mu)^r\right] = \frac{1}{N}\sum_{i=1}^{N} sign(x_i-\mu)((x_i-\mu)^2)^{r/2} \tag{8}$$

$$sign(x_i-\mu) = \begin{cases} 1, x_i-\mu \geq 0 \\ 0, x_i-\mu = 0 \\ -1, x_i-\mu < 0 \end{cases} \tag{9}$$

According to these definitions, the fractional-order moment A with order 4 is the same with kurtosis and the fractional-order moment B with the order 3 is the same with skewness. The moment A with order 2 is equal to 1 and the moment B with order 1 is equal to 0. In the following we will not consider these two constants.

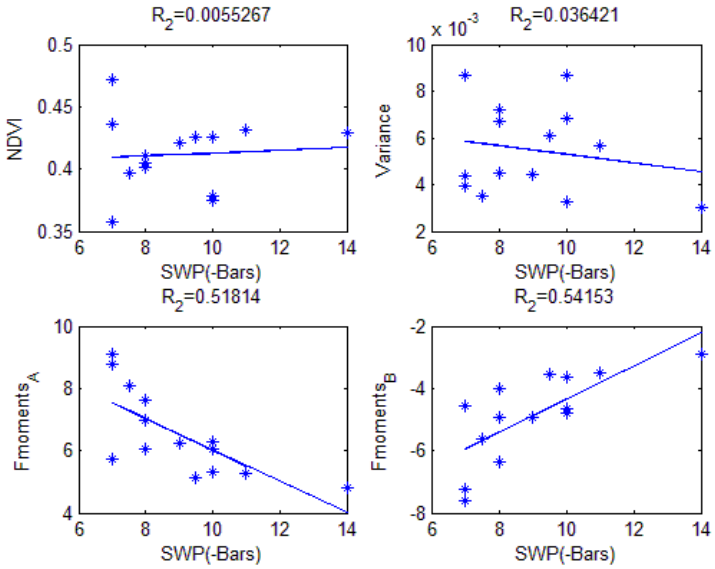

Figure 3. Correlation between SWP and mean, variance, fractional-order moments using method A and method B of order 5, in middle block on June 12, 2015

Results and Discussions

We compared four different methods to extract water stress signature from images, NDVI mean, NDVI variance, fractional-order moments of DN difference between the NIR band and the blue band of every pixel within canopies obtained using the method A and the method B, denoted as fractional-order moment A ($Fmoment_A$) and fractional-order moment B($Fmoment_B$). The optimal order of the moments was determined by grid search within the range of [0.2, 10] with the step 0.2.

Fig. 3, 5, 6 showed the scatter plots, fitted lines, and R square between SWP and extracted vegetation indices of three different days, June 12, June 18, and August 20, 2015 in the middle block, where the x axis is SWP, and the y axis stands for the extracted vegetation indices from the image.

According to Fig. 4, the correlation between fractional-order moments and SWP, quantified by R square, can be tuned by changing the order. By definition, the fractional-order moment A with order 2 is always 1, since it is standardized. The fractional-order moment with order 1 is always 0. So these two points were marked with circles in Fig. 4. When the order is changed from 0.2 to 10, first the R square is increased and then it is decreased. There is an optimal order where the R square is the largest. It is interesting that the optimal order is not at the integer point. The optimal order for moment A is 5 and the optimal order for moment B is 4.4. The performances of moment A and moment B were not exactly the same. Therefore, the value of moments order in Fig. 3, 5, 6 are not the one yielding best R square at the same time, but the one yielding relatively good R square with both moments A and moments B. According to Fig. 3, 5, 6, it is shown that moments-based methods perform better than NDVI mean and variance.

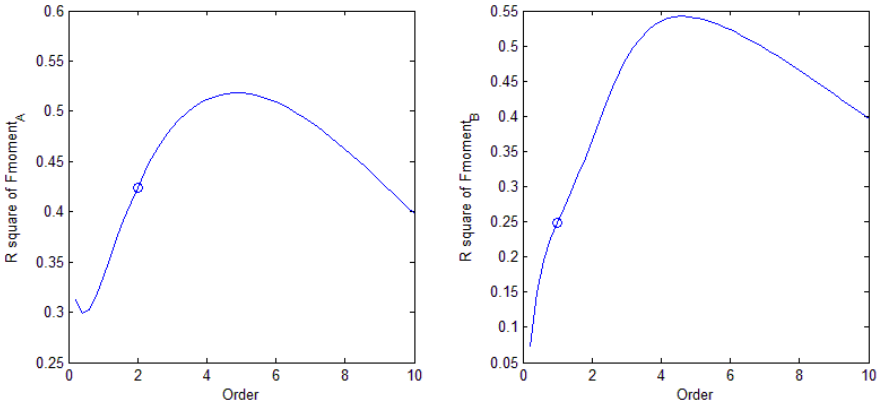

Figure 4. R square vs. order of the fractional-order moments, in middle block, on June 12, 2015

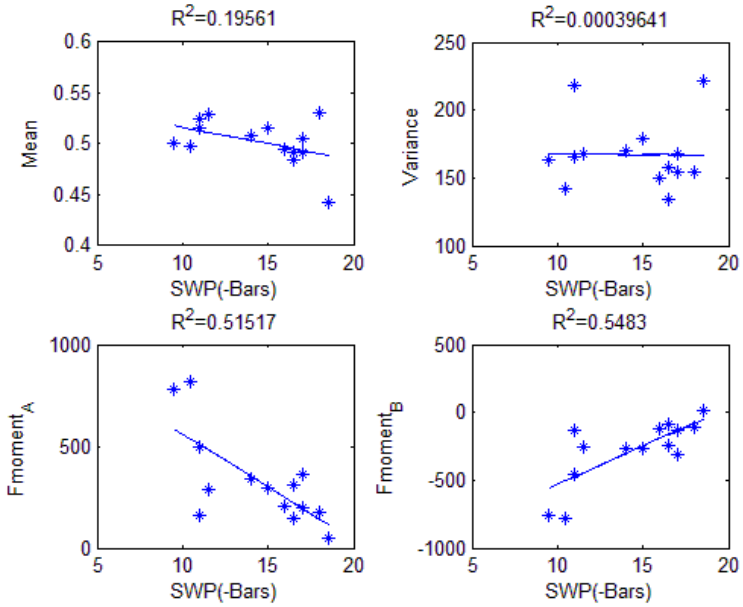

Figure 5. Correlation between SWP and mean, variance, fractional-order moments using method A and method B of order 10, in middle block on June 18, 2015

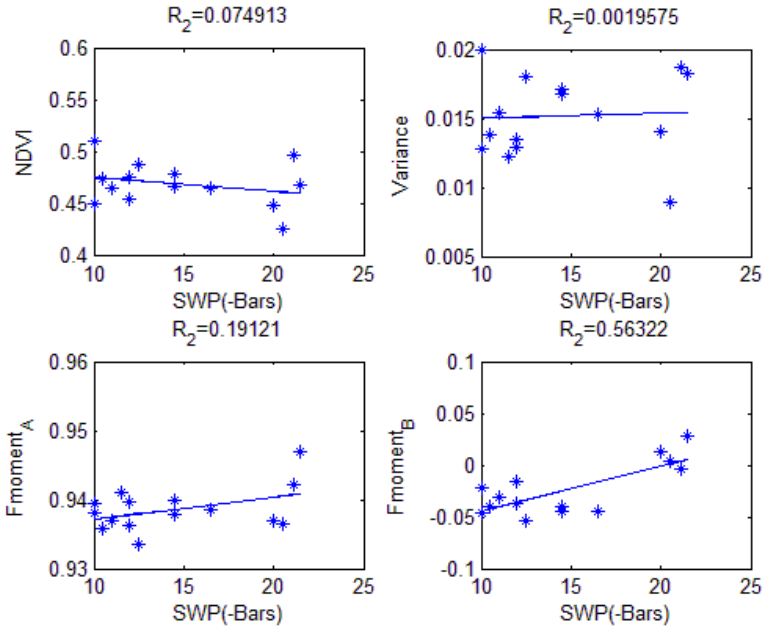

Figure 6. Correlation between SWP and mean, variance, fractional-order moments using method A and method B of order 1.8, in middle block on August 20, 2015

Conclusions

With the development of UAV and camera technologies, it becomes much easier to collect high resolution images with affordable cost and flexible timing. Yet the challenge is to make sense of these high resolution images to obtain accurate information. Based on past work on non-normalized difference vegetation indices (Zhao, Stark, Chen, Ray, & Doll, 2016), we discussed the best order of fractional-order moments. Performances of traditional NDVI mean, NDVI variance and fractional-order moments of canopy difference were compared. Fractional-order moments improved the correlation between image-based results and SWP, and the optimal order of fractional-order moments was not an integer but a fraction.

Acknowledgements

Thanks to Andrew Ray for field measurements and Larry Burrow for lending his expertise in almond orchard. Thanks to MESA Lab Scientific Data Drone crew members Ph.D. students Brandon Stark and Brendan Smith, undergraduate researchers Yoni Shchemelinin, Andreas Anderson, Jacob Clark, Allan Murillo for contributions in conducting flight missions in the 2015 growing season.

References

Agam, N., Segal, E., Peeters, A., Levi, A., Dag, A., Yermiyahu, U., & Ben-Gal, A. (2014). Spatial distribution of water status in irrigated olive orchards by thermal imaging. *Precision agriculture, 15*, 346-359.

Allen, R. G., Pereira, L. S., Raes, D., Smith, M., & others. (1998). Crop evapotranspiration-Guidelines for computing crop water requirements-FAO Irrigation and drainage paper 56. *FAO, Rome, 300*, D05109.

Bellvert, J., Marsal, J., Girona, J., Gonzalez-Dugo, V., Fereres, E., Ustin, S. L., & Zarco-Tejada, P. J. (2016). Airborne thermal imagery to detect the seasonal evolution of crop water status in peach, nectarine and Saturn peach orchards. *Remote Sensing, 8*, 39.

Candiago, S., Remondino, F., De Giglio, M., Dubbini, M., & Gattelli, M. (2015). Evaluating multispectral images and vegetation indices for precision farming applications from UAV images. *Remote Sensing, 7*, 4026-4047.

Dhillon, R., Francisco, R. O., Roach, J., Upadhyaya, S., & Delwiched, M. (2014). A continuous leaf monitoring system for precision irrigation management in orchard crops. *Tar{\i}m Makinalar{\i} Bilimi Dergisi, 10*.

Doll, D., & Shackel, K. (2016). Drought management for California almonds. *Crops and Soils, 49*, 28-35.

Fulton, A., Grant, J., Buchner, R., & Connell, J. (2014). Using the pressure chamber for irrigation management in walnut, almond, and prune. *Oakland: University of California Division of Agriculture and Natural Resources Publication, 8503*.

Goldhamer, D. A., Fereres, E., Mata, M., Girona, J., & Cohen, M. (1999). Sensitivity of continuous and discrete plant and

soil water status monitoring in peach trees subjected to deficit irrigation. *Journal of the American Society for Horticultural Science, 124*, 437-444.

Gonzalez-Dugo, V., Goldhamer, D., Zarco-Tejada, P. J., & Fereres, E. (2015). Improving the precision of irrigation in a pistachio farm using an unmanned airborne thermal system. *Irrigation Science, 33*, 43-52.

Gonzalez-Dugo, V., Zarco-Tejada, P., Berni, J. A., Suárez, L., Goldhamer, D., & Fereres, E. (2012). Almond tree canopy temperature reveals intra-crown variability that is water stress-dependent. *Agricultural and Forest Meteorology, 154*, 156-165.

Khanal, S., Fulton, J., & Shearer, S. (2017). An overview of current and potential applications of thermal remote sensing in precision agriculture. *Computers and Electronics in Agriculture, 139*, 22-32.

Matese, A., Toscano, P., Gennaro, D. a., Genesio, L., Vaccari, F. P., Primicerio, J., . . . Gioli, B. (2015). Intercomparison of UAV, aircraft and satellite remote sensing platforms for precision viticulture. *Remote Sensing, 7*, 2971-2990.

Mekonnen, M. M., & Hoekstra, A. Y. (2016). Four billion people facing severe water scarcity. *Science advances, 2*, e1500323.

Nigmatullin, R. R. (2006). The statistics of the fractional moments: Is there any chance to "read quantitatively" any randomness? *Signal Processing, 86*, 2529-2547.

Nilsson, H. (1995). Remote sensing and image analysis in plant pathology. *Annual review of phytopathology, 33*, 489-528.

Shackel, K. A., Ahmadi, H., Biasi, W., Buchner, R., Goldhamer, D., Gurusinghe, S., . . . others. (1997). Plant water status as an index of irrigation need in deciduous fruit trees. *HortTechnology, 7*, 23-29.

Shackel, K., Edstrom, J., Fulton, A., Lampinen, B., Schwankl, L., Olivos, A., . . . others. (2011). Drought survival strategies for established almond orchards on shallow soil. *Modesto, CA, 2012*.

Shackel, K., Lampinen, B., Sibbett, S., Olson, W., & others. (2000). The relation of midday stem water potential to the growth and physiology of fruit trees under water limited conditions. *Acta Horticulturae*, 425-430.

Slayter, R. O., & others. (1967). Plant-water relationships. *Plant-water relationships.*

Smith, G. M., & Milton, E. J. (1999). The use of the empirical line method to calibrate remotely sensed data to reflectance. *International Journal of remote sensing, 20*, 2653-2662.

Stark, B., Zhao, T., & Chen, Y. (2016). An analysis of the effect of the bidirectional reflectance distribution function on remote sensing imagery accuracy from small unmanned aircraft systems. *Unmanned Aircraft Systems (ICUAS), 2016 International Conference on*, (pp. 1342-1350).

Steduto, P., Hsiao, T. C., Fereres, E., & Raes, D. (2012). *Crop yield response to water.* FAO Roma.

Suárez, L., Zarco-Tejada, P. J., González-Dugo, V., Berni, J. A., & Fereres, E. (2008). Detecting water stress in orchard crops using PRI from airborne imagery. *6th EARSeL SIG IS workshop imaging Spectroscopy: Innovative tool for scientific and commercial environmental applications, March 16--19, 2009, Tel-Aviv, Israel.*

Wang, D., Gartung, J. (2010). Infrared canopy temperature of early-ripening peach trees under postharvest deficit irrigation. *Agricultural Water Management* 97, 1787-1794.

Yang, Q., Chen, D., Zhao, T., & Chen, Y. (2016). Fractional calculus in image processing: a review. *Fractional Calculus and Applied Analysis, 19*, 1222-1249.

Zhao, T., Stark, B., Chen, Y., Ray, A. L., & Doll, D. (2015). A detailed field study of direct correlations between ground truth crop water stress and normalized difference vegetation index (NDVI) from small unmanned aerial system (sUAS). *Unmanned Aircraft Systems (ICUAS), 2015 International Conference on*, (pp. 520-525).

Zhao, T., Stark, B., Chen, Y., Ray, A. L., & Doll, D. (2016). Challenges in water stress quantification using small unmanned aerial system (sUAS): Lessons from a growing season of almond. *Unmanned Aircraft Systems (ICUAS), 2016 International Conference on*, (pp. 1366-1370).

Zhao, T., Stark, B., Chen, Y., Ray, A., & Doll, D. (2016). More Reliable Crop Water Stress Quantification Using Small Unmanned Aerial Systems (sUAS). *IFAC-PapersOnLine, 49*, 409-414.

Zhao, T., Wang, Z., Yang, Q., & Chen, Y. (2017). Melon yield prediction using small unmanned aerial vehicles. *SPIE Commercial+ Scientific Sensing and Imaging*, (pp. 1021808-1021808).

Zheng, H., Zhou, X., Cheng, T., Yao, X., Tian, Y., Cao, W., & Zhu, Y. (2016). Evaluation of a UAV-based hyperspectral frame camera for monitoring the leaf nitrogen concentration in rice. *Geoscience and Remote Sensing Symposium (IGARSS), 2016 IEEE International*, (pp. 7350-7353).